Article

Catalytic Roles of Active-Site Amino Acid Residues of Coenzyme B-Dependent Diol Dehydratase: Protonation State of Histidine and Pull Effect of Glutamate

Takashi Kamachi, Tetsuo Toraya, and Kazunari Yoshizawa

J. Am. Chem. Soc., **2004**, 126 (49), 16207-16216• DOI: 10.1021/ja045572o • Publication Date (Web): 18 November 2004

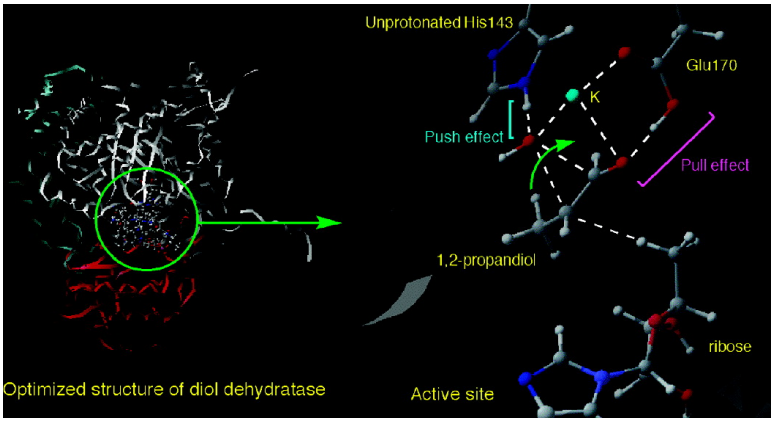

More About This Article

Additional resources and features associated with this article are available within the HTML version:

- Supporting Information
- Links to the 4 articles that cite this article, as of the time of this article download
- Access to high resolution figures
- Links to articles and content related to this article
- Copyright permission to reproduce figures and/or text from this article

View the Full Text HTML

J|A|C|S
ARTICLES
Published on Web 11/18/2004

Catalytic Roles of Active-Site Amino Acid Residues of Coenzyme B_{12}-Dependent Diol Dehydratase: Protonation State of Histidine and Pull Effect of Glutamate

Takashi Kamachi,[†] Tetsuo Toraya,*[,‡] and Kazunari Yoshizawa*[,†]

Contribution from the Institute for Materials Chemistry and Engineering, Kyushu University, Fukuoka 812-8581, Japan, Department of Bioscience and Biotechnology, Okayama University, Okayama 700-8530, Japan

Received July 23, 2004; E-mail: kazunari@ms.ifoc.kyushu-u.ac.jp; toraya@cc.okayama-u.ac.jp

Abstract: The hydrogen abstraction and the OH migration processes catalyzed by diol dehydratase are discussed by means of a quantum mechanical/molecular mechanical method. To evaluate the push effect of His143 and the pull effect of Glu170, we considered three kinds of whole-enzyme model, the protonated and two unprotonated His143 models. A calculated activation energy for the hydrogen abstraction by the adenosyl radical is 15.6 (13.6) kcal/mol in the protonated (unprotonated) His143 model. QM/MM calculational results show that the mechanism of the OH migration is significantly changed by the protonation of His143. In the protonated His143 model, the OH group migration triggered by the full proton donation from the imidazolium to the migrating OH group occurs by a stepwise OH abstraction/re-addition process in which the water production reduces the barrier for the C−O bond cleavage. On the other hand, the OH migration in the unprotonated His143 model proceeds in a concerted manner, as we previously proposed using a simple model including only K^+ ion and substrate. The latter mechanism seems to be kinetically more favorable from the calculated energy profiles and is consistent with experimental results. The activation barrier of the OH group migration step is only 1.6 kcal/mol reduced by the hydrogen-bonding interaction between the O2 of the substrate and unprotonated His143. Thus, it is predicted that His143 is not protonated, and therefore the main active-site amino acid residue that lowers the energy of the transition state for the OH group migration is determined to be Glu170.

1. Introduction

Coenzyme B_{12} or adenosylcobalamin (AdoCbl) is an essential cofactor for several enzymes, such as diol dehydratase, ethanolamine ammonia lyase, and methylmalonyl-CoA mutase.[1,2] The coenzyme has a unique covalent bond between cobalt and C5′ of the adenosyl group, which is a rare example of a naturally occurring organometallic compound. A common feature of AdoCbl-dependent reactions is the migration of a hydrogen atom from one carbon atom of substrate to an adjacent carbon atom in exchange for group X, as shown in Chart 1.

Chart 1

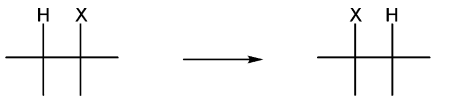

X = $CH(NH_3^+)COO^-$, $C(=CH_2)COO^-$, COSCoA, OH, NH_3^+

Diol dehydratase[2] catalyzes the conversion of 1,2-diols to the corresponding aldehydes. Figure 1 shows a minimal mechanism

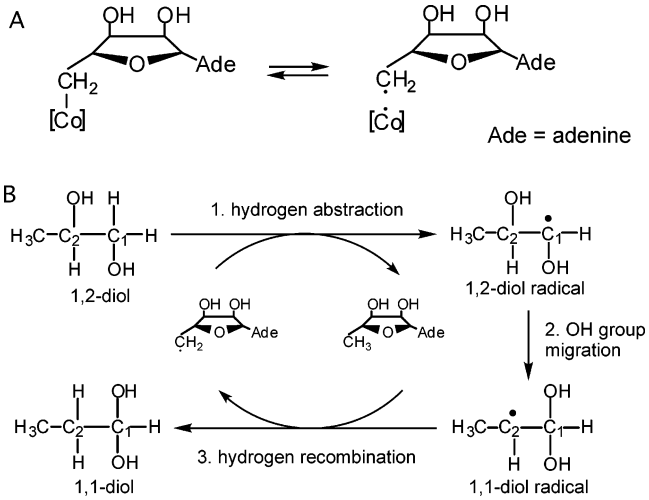

Figure 1. Minimal mechanism of the diol dehydratase reaction. (A) Homolytic cleavage of the Co−C bond in AdoCbl. (B) Adenosyl radical-catalyzed rearrangement.

for this enzymatic dehydration that involves the hydrogen atom abstraction from C1 and the migration of an OH group from C2 to C1 of 1,2-propanediol. The adenosyl ($AdoCH_2$) radical that is generated by the homolytic cleavage of the Co−C covalent bond in AdoCbl plays an essential role in this OH group migration and thus effectively promotes this chemically difficult

[†] Institute for Materials Chemistry and Engineering, Kyushu University.
[‡] Department of Bioscience and Biotechnology, Okayama University.

(1) (a) Dolphin, D., Ed. In *B_{12}*; John Wiley & Sons: New York, 1982; Vol. 2. (b) Banerjee, R., Ed. In *Chemistry and Biochemistry of B_{12}*; John Wiley & Sons: New York, 1999.
(2) (a) Toraya, T. *Chem. Rev.* **2003**, *103*, 2095. (b) Toraya, T. *Cell. Mol. Life Sci.* **2000**, *57*, 106.

reaction. At first, the adenosyl radical abstracts a hydrogen atom from C1 to form 1,2-diol radical (substrate-derived radical), and then the OH group on C2 migrates to C1 leading to the formation of 1,1-diol radical (product-related radical). The resultant 1,1-diol radical abstracts a hydrogen atom from 5′-deoxyadenosine ($AdoCH_3$), which leads to the formation of the 1,1-diol and the regeneration of $AdoCH_2$ radical.

Recent crystal structure analyses of the complexes of diol dehydratase with cyanocobalamin and adeninylpentylcobalamin showed that both hydroxyl groups of substrate coordinate directly to K^+ ion at the active site, which implies the participation of K^+ ion in the OH group migration.[3] On the basis of the crystal structures, a possible mechanism of action of diol dehydratase has been proposed.[2a,3] To reveal the catalytic roles of K^+ ion in the diol dehydratase reaction, we performed density-functional-theory (DFT) calculations with a simple model involving K^+ ion, propanediol, and ethyl radical.[4−6] It was considered that in the course of the reaction the substrate and the radical intermediates are always bound to K^+ ion until the release of product aldehyde from the active site and that the OH group migration proceeds in a concerted manner with the aid of K^+ ion. These results suggest that the most important role of K^+ ion in the reaction is to fix the substrate and the intermediates in proper position in order to ensure the hydrogen abstraction and recombination. However, the lowering of the activation energy by K^+ ion for the OH group migration is only 2.2 kcal/mol, and thus the transition state for the OH group migration is calculated to be energetically higher than that for the hydrogen atom abstraction. This result is inconsistent with the observed large deuterium kinetic isotope effects (KIEs) that indicate the involvement of hydrogen atom transfer in the rate-determining step for the overall reaction.[7−9] The main reason for this discrepancy is that the contributions of active-site amino acid residues to the OH group migration were not taken into consideration in our previous calculations. Golding and Radom proposed from ab initio molecular orbital calculations that the barrier of the OH group migration is decreased by the partial protonation of the migrating OH group.[10] For example, the partial proton transfer from NH_4^+ and $CH_3OH_2^+$ to the migrating OH group lowers the activation barrier for the OH migration of the 1,2-dihydroxyethyl radical by 15.2 and 26.4 kcal/mol, respectively.[10c] Moreover, they demonstrated that the barrier height for the transition state can be further reduced by partial deprotonation of the spectator OH group (5.7 kcal/mol by HCO_2^-).[10d] Their proposals are in good agreement with the experimental results using site-directed mutagenesis that Glu170Ala mutant of diol dehydratase is totally inactive and the His143Ala mutant shows only a trace of enzymatic activity.[2a,11]

In this study, we describe the hydrogen atom abstraction and the OH group migration processes catalyzed by diol dehydratase from a quantum mechanical/molecular mechanical method, which is a powerful approach to treat a large molecular system with a relatively modest computational task. These calculations are based on the following assumptions: (i) Glu170 is ionized at the start of the reaction, and (ii) K^+ ion remains coordinated to the substrate and all radical intermediates throughout the course of the reaction. The main aim of this study is to address how the protein environment of diol dehydratase contributes to the hydrogen atom abstraction and the OH group migration in the dehydration reaction.

2. Method of Calculation

We built an entire model of diol dehydratase based on the crystal structure (PDB ID 1EEX) of diol dehydratase-adeninylpentylcobalamin (AdePeCbl) complex as discussed in detail in section 3−1. To make the realistic enzyme model for QM/MM calculations, missing hydrogen atoms were added and then initial MM minimization was performed while the QM region was fixed. The completed model with about 13 500 atoms was used as an initial structure for the QM/MM calculation with a two-layer ONIOM (IMOMM) method[12] implemented in the Gaussian 98 program.[13] In these calculations, a specified region around the active site was calculated with a QM method, while the rest of the protein was treated at an MM level. The QM region can describe the essential bond-breaking and bond-making processes in the enzyme, whereas the MM region can promote interactions with the QM region through partial charges and van der Waals forces of atoms in the MM region. At the QM/MM border, atoms in the MM region bound to an atom in the QM region are replaced by hydrogen atoms during the QM-level part of the QM/MM calculation.

Figure 2 shows an optimized structure of the enzyme model and the all heavy atoms in the QM region. K^+ ion is coordinated by five oxygen atoms originated from the side chain of Gln141, Glu170, Glu221, Gln296, and the carbonyl group of Ser362. The sixth and seventh coordination positions are occupied by O1 and O2 of substrate (*S*)-1,2-propanediol (PDO); the *S*-enantiomer is preferred in the binding by the enzyme.[14,15] The ribose moiety of 5′-deoxyadenosyl radical and the side chain of His143 are also involved in the QM region. The QM

(3) (a) Shibata, N.; Masuda, J.; Tobimatsu, T.; Toraya, T.; Suto, K.; Morimoto, Y.; Yasuoka, N. *Structure* **1999**, *7*, 997. (b) Masuda, J.; Shibata, N.; Morimoto, Y.; Toraya, T.; Yasuoka, N. *Structure* **2000**, *8*, 775. (c) Shibata, N.; Masuda, J.; Morimoto, Y.; Yasuoka, N.; Toraya, T. *Biochemistry* **2002**, *41*, 12617. (d) Shibata, N.; Nakanishi, Y.; Fukuoka, M.; Yamanishi, M.; Yasuoka, N.; Toraya, T. *J. Biol. Chem.* **2003**, *278*, 22717.
(4) Toraya, T.; Yoshizawa, K.; Eda, M.; Yamabe, T. *J. Biochem.* (*Tokyo*) **1999**, *126*, 650.
(5) Toraya, T.; Eda, M.; Kamachi, T.; Yoshizawa, K. *J. Biochem.* (*Tokyo*) **2001**, *130*, 865.
(6) Eda, M.; Kamachi, T.; Yoshizawa, K.; Toraya, T. *Bull. Chem. Soc. Jpn.* **2002**, *75*, 1469.
(7) Eagar, R. G. Jr.; Bachovchin, W. W.; Richards, J. H. *Biochemistry* **1975**, *14*, 5523−5528.
(8) Essenberg, M. K.; Frey, R. A.; Abeles, R. H. *J. Am. Chem. Soc.* **1971**, *93*, 1242−1251.
(9) (a) Frey, P. A.; Karabatsos, G. L.; Abeles, R. H. *Biochem. Biophys. Res. Commun.* **1965**, *18*, 551−556. (b) Zagalak, B.; Frey, P. A.; Karabatsos, G. L.; Abeles, R. H. *J. Biol. Chem.* **1966**, *241*, 3028−3035.
(10) (a) Golding, B. T.; Radom, L. *J. Chem. Soc., Chem. Commun.* **1973**, 939. (b) Golding, B. T.; Radom, L. *J. Am. Chem. Soc.* **1976**, *98*, 6331. (c) Smith, D. M.; Golding, B. T.; Radom, L. *J. Am. Chem. Soc.* **1999**, *121*, 5700. (d) Smith, D. M.; Golding, B. T.; Radom, L. *J. Am. Chem. Soc.* **2001**, *123*, 1664.
(11) In this paper, all residue numbers in the α subunit.
(12) (a) Maseras, F.; Morokuma, K. *J. Comput. Chem.* **1995**, *16*, 1170. (b) Humbel, S.; Sieber, S.; Morokuma, K. *J. Chem. Phys.* **1996**, *105*, 1959. (c) Matsubara, T.; Sieber, S.; Morokuma, K. *Int. J. Quant. Chem.* **1996**, *60*, 1101. (d) Svensson, M.; Humbel, S.; Froese, R. D. J.; Matsubara, T.; Sieber, S.; Morokuma, K. *J. Phys. Chem.* **1996**, *100*, 19357. (e) Svensson, M.; Humbel, S.; Morokuma, K. *J. Chem. Phys.* **1996**, *105*, 3654. (f) Dapprich, S.; Komáromi, I.; Byun, K. S.; Morokuma, K.; Frisch, M. J. *J. Mol. Struct. (THEOCHEM)* **1999**, *461−462*, 1. (g) Vreven, T.; Morokuma, K. *J. Comp. Chem.* **2000**, *21*, 1419.
(13) Frisch, M. J.; Trucks, G. W.; Schlegel, H. B.; Scuseria, G. E.; Robb, M. A.; Cheeseman, J. R.; Zakrzewski, V. G.; Montgomery, J. A.; Stratmann, R. E.; Burant, J. C.; Dapprich, S.; Millam, J. M.; Daniels, A. D.; Kudin, K. N.; Strain, M. C.; Farkas, O.; Tomasi, J.; Barone, V.; Cossi, M.; Cammi, R.; Mennucci, B.; Pomelli, C.; Adamo, C.; Clifford, S.; Ochterski, J.; Petersson, G. A.; Ayala, P. Y.; Cui, Q., Morokuma, K.; Malick, D. K.; Rabuck, A. D.; Raghavachari, K.; Foresman, J. B.; Cioslowski, J.; Ortiz, J. V.; Stefanov, B. B.; Liu, G.; Liashenko, A.; Piskorz, P.; Komaromi, I.; Gomperts, R.; Martin, R. L.; Fox, D. J.; Keith, T.; Al-Laham, M. A.; Peng, C. Y.; Nanayakkara, A.; Gonzalez, C.; Challacombe, M.; Gill, P. M. W.; Johnson, B.; Chen, W.; Wong, M. W.; Andres, J. L.; Gonzalez, C.; Head-Gordon, M.; Replogle, E. S.; Pople, J. A. *Gaussian 98*; Gaussian Inc.: Pittsburgh, PA, 1998.
(14) Bachovchin, W. W.; Eagar, R. G. Jr.; Moore, K. W.; Richards, J. H. *Biochemistry* **1977**, *16*, 1082.
(15) Yamane, T.; Kato, T.; Shimizu, S.; Fukui, S. *Arch. Biochem. Biophys.* **1966**, *113*, 362.

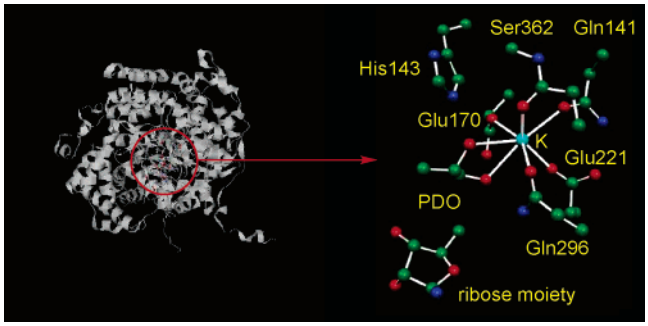

Figure 2. Diol dehydratase model with 13 500 atoms. The QM region includes the ribose moiety, K^+ ion, PDO, and truncated models of Gln141, His143, Glu170, Glu221, Gln296, and Ser362.

calculation is performed with the B3LYP method, which consists of the Slater exchange, the Hartree−Fock exchange, the exchange functional of Becke,[16] the correlation functional of Lee, Yang, and Parr (LYP),[17] and the correlation functional of Vosko, Wilk, and Nusair.[18] To carry out geometry optimizations, we used the 6-31G* basis set[19,20] for K, PDO, ribose moiety, and amino acid residues that directly interact with PDO through hydrogen bonds (His143, Glu170, Gln296), and we used the 3-21G basis set[21] for the rest amino acid residues (Gln141, Glu221, and Ser362). We used the 6-311++G** basis set[22,23] of Pople and co-workers for C, O, N, and H, and the primitive set of Wachters[24] for K[25] to compute single-point energies at a higher level. DFT methods have been extensively used for the study of radical reactions and hydrogen-bonded systems.[26−29] The reliability of this method for the present system is shown in the Supporting Information. The relative energies between some intermediates are insensitive to the choice of functionals, and the BSSE[30,31] effect is very small. The method of choice for MM calculations is the amber force field (Amber96).[32] We modified the Gaussian 98 program to allow for external definition of atom types and parameters for cobalamin developed by Marques et al.[33] These data are listed in the Supporting Information. All calculations were performed with 3.0 GHz personal computers (PC).

3. Results and Discussion

The interaction of the migrating OH group with the imidazolium ion of His143 has been considered to be essential for the stabilization of the transition state for the OH migration. Smith, Golding, and Radom demonstrated that partial proton transfer to the migrating OH group from a range of Brønsted acids weakens the C−O bond leading to barrier reduction.[10] The X-ray structure of the active site reveals that the OH group on C2 of substrate is hydrogen-bonded to His143.[3] However, this catalytic mechanism should be reevaluated because the rate of diol dehydratase reaction is constant in a pH range from 6.0 to 10.0.[34] Is the protonated His143 residue essential or not? To address this question, we considered three whole-enzyme models of diol dehydratase-AdoCbl complex with protonated and unprotonated His143 for the purpose of comparison. These models differ in the protonation state: a hydrogen atom is connected to ϵ-nitrogen (Nϵ2) or δ-nitrogen (Nδ1) atom of the His143 residue in the unprotonated His143 model, while a hydrogen atom is connected to both nitrogen atoms in the protonated His143 model. We mainly discuss structures, electronic properties, and energetics of the protonated His143 model and the unprotonated His143 model with a hydrogen atom connected to the ϵ-nitrogen (Nϵ2) atom (HIE) because only ϵ-nitrogen of His143 can contribute to the binding of the substrate and the stabilization of the transition state for the OH migration via a hydrogen-bonding interaction. Detailed data on calculational results of the unprotonated His143 model with a hydrogen atom connected to the δ-nitrogen atom (HID or normal histidine) is collected in Supporting Information. QM/MM calculations using these models have successfully provided important clues to evaluate the catalytic roles of the Glu170 and His143 residues in the OH group migration.

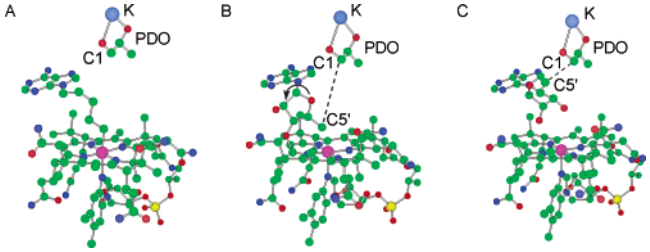

Figure 3. Active site structure of diol dehydratase. (A) X-ray structure of the diol dehydratase-AdePeCbl complex. (B) Diol dehydratase−AdoCbl model complex produced by replacing the pentyl moiety of A with ribose. (C) Optimized structure of the diol dehydratase−AdoCbl complex model after the rotation of the ribose moiety.

3-1. Ribosyl Rotation for Radical Transfer from AdoCbl to Substrate. Adeninylethylcobalamin (AdeEtCbl) can promote the Co−C cleavage upon binding to apodiol dehydratase, whereas adeninylpropylcobalamin (AdePrCbl) and other longer chain homologues cannot.[35] On the basis of these results, the adenine-attracting effect of apoenzyme is proposed as a major element that weakens the Co−C bond. The presence of the adenine-binding site in diol dehydratase was recently ascertained by the crystal structure analysis of the diol dehydratase−AdePeCbl complex.[3b] The crystal structure shows that the adenine moiety of this analogue is trapped by a hydrogen-bonding network with a water molecule and surrounding amino acid residues, Ser224, Ser299, Ser301, and Gly261. As shown in Figure 3A, the adenine-binding pocket fixes the adenine ring to allow tight binding of adenylpentyl group to the Co atom at a distance of 1.89 Å, which is the main reason for the catalytic inactivity of the analogue.

(16) (a) Becke, A. D. *Phys. Rev. A* **1988**, *38*, 3098. (b) Becke, A. D. *J. Chem. Phys.* **1993**, *98*, 5648.
(17) Lee, C.; Yang, W.; Parr, R. G. *Phys. Rev. B* **1988**, *37*, 785.
(18) Vosko, S. H.; Wilk, L.; Nusair, M. *Can. J. Phys.* **1980**, *58*, 1200.
(19) (a) Ditchfield, R.; Hehre, W. J.; Pople, J. A. *J Chem. Phys.* **1971**, *54*, 724. (b) Hehre, W. J.; Ditchfield, R.; Pople, J. A. *J Chem. Phys.* **1972**, *56*, 2257. (c) Hariharan, P. C.; J. A. Pople. *Theoret. Chim. Acta.* **1973**, *28*, 213.
(20) Rassolov, V. A.; Pople, J. A.; Ratner, M. A.; Windus, T. L. *J Chem. Phys.* **1998**, *109*, 1223.
(21) Binkley, J. S.; Pople, J. A.; Hehre, W. J. *J. Am. Chem. Soc.* **1980**, *102*, 939.
(22) Krishnan, R.; Binkley, J. S.; Seegar, R.; Pople, J. A. *J. Chem. Phys.* **1980**, *72*, 650.
(23) Clark, T.; Chandrasekhar, J.; Spitznagel, G. W.; Schleyer, P. v. R. *J. Comp. Chem.* **1983**, *4*, 294.
(24) Wachters, A. J. H. *J. Chem. Phys.* **1970**, *52*, 1033−1036.
(25) A (62111111|3311111|31) [8s7p2d] contraction. This is the same as a standard parameter of Gaussian 98 ab initio program for K at the 6-311G* level of theory.
(26) Basch, H.; Hoz, S. *J. Phys. Chem. A* **1997**, *101*, 4416.
(27) Pérez-Casany, M. P.; Nebot-Gil, I.; Sánchez-Marín, J. *J. Phys. Chem. A* **2000**, *104*, 10721.
(28) Lozynski, M.; Rusinska-Roszak, D.; Mack, H.-G. *J. Phys. Chem. A* **1998**, *102*, 2899.
(29) Müller-Dethlefs, K.; Hobza, P. *Chem. Rev.* **2000**, *100*, 143.
(30) Boys, S. F.; Bernardi, F.; *Mol. Phys.* **1970**, *19*, 553.
(31) Simon, S.; Duran, M.; Dannenberg, J. J. *J. Chem. Phys.* **1996**, *105*, 11024.
(32) Cornell, W. D.; Cieplak, P.; Bayly, C. I.; Gould, I. R.; Merz, K. M., Jr.; Ferguson, D. M.; Spellmeyer, D. C.; Fox, T.; Caldwell, J. W.; Kollman, P. A. *J. Am. Chem. Soc.* **1995**, *117*, 5179.
(33) Marques, H. M.; Ngoma, B.; Egan, T. J.; Brown, K. L. *J. Mol. Struct.* **2001**, *561*, 71.
(34) Lee, H. A.; Abeles, R. H. *J. Biol. Chem.* **1963**, *238*, 2367.
(35) Toraya, T.; Watanabe, N.; Ichikawa, M.; Matsumoto, T.; Ushio, K.; Fukui, S. *J. Biol. Chem.* **1987**, *262*, 8544.

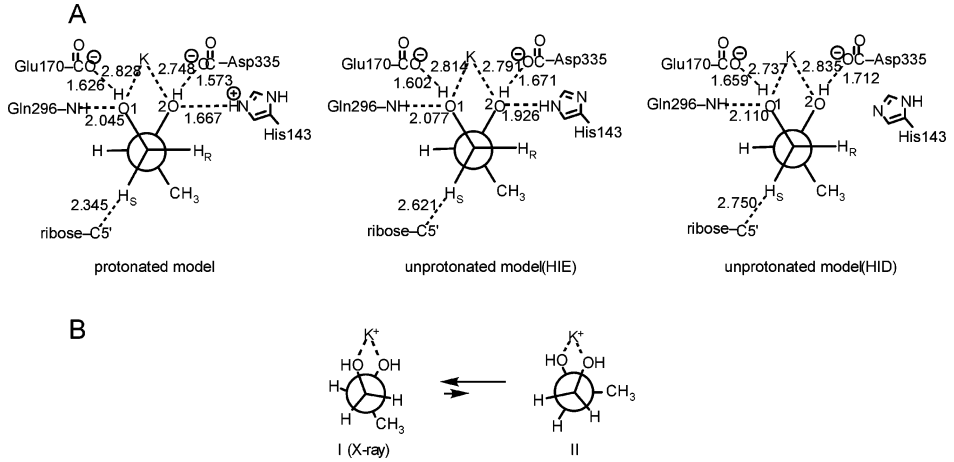

Figure 4. Binding of (*S*)-1,2-propanediol to K^+ ion. (A) The hydrogen-bonding network between the substrate and surrounding amino acid residues in the optimized structures of protonated and unprotonated models. Units in Å. (B) Interconversion between two possible conformations I and II.

Abeles's[36] and Rétey's[37] groups demonstrated from labeling experiments that the *pro-S* hydrogen atom on the C1 atom of (*S*)-1,2-propanediol stereospecifically migrates to the C2 atom. How can C5′-centered radical of the adenosyl group abstract the specific hydrogen atom from the substrate? Toraya and co-workers[3b] demonstrated using a modeling study of X-ray structure of the diol dehydratase−AdePeCbl complex that the aforementioned adenine-binding site is functionally relevant to the Co−C bond cleavage and the stereospecific hydrogen abstraction by the adenosyl radical. Figure 3B shows the diol dehydratase−AdoCbl model complex whose structure is produced from the diol dehydratase−AdePeCbl complex only by replacing the pentyl moiety with ribose. While keeping the position of the adenine ring, we elongated the bond distance between the C5′ carbon of the ribose moiety and the Co atom to 3.3 Å, which means that marked strains induced by the constraint of the adenine ring position cleave the Co−C bond. The Co−C bond dissociation energy of coenzyme B_{12} has been estimated to be about 30 kcal/mol from experimental[38,39] and theoretical studies.[40−44] Thus, the steric strain induced by the interaction between the cobalamin moiety and the adenine ring is considered to be sufficient to accelerate the cleavage of the weak Co−C bond. The C1 atom of the substrate is 6.6 Å apart from the radical center C5′ in the AdoCbl model. Although this distance is too far for the radical transfer from the substrate to the adenosyl radical, the C5′-centered radical of the adenosyl group becomes accessible to the *pro-S* hydrogen atom on C1 of the substrate by rotating the ribose moiety around the glycosidic linkage. Figure 3C shows an optimized structure of the diol dehydratase-AdoCbl complex after the rotation of the ribose moiety (reactant complex). The distances from C5′ to C1 and C2 of the substrate are 3.128 and 4.091 Å, respectively. The *pro-S* hydrogen atom to be abstracted is on the same side as the adenosyl group and close to C5′, whereas the *pro-R* hydrogen is positioned in a different direction and far from the radical center. These structural features enable the stereospecific hydrogen abstraction from C1.

3-2. Substrate-Binding Site Around K^+ Ion. Let us next look at the substrate-binding site around K^+ ion involving a complex hydrogen-bonding network in which the hydrogen abstraction and the OH group migration proceed. Figure 4A shows a schematic representation of the hydrogen-bonding network between (*S*)-1,2-propanediol and surrounding amino acid residues with optimized parameters from QM/MM calculations of the whole-enzyme models with protonated and unprotonated His143. The OH groups of substrate coordinate to K^+ ion in order to fix the substrate in the proper positions at the active site, as previously proposed. There is an argument whether K^+ ion in the active site remains coordinated to the substrate and all radical intermediates throughout the course of the reaction. Frey and co-workers have reported that both EPR and pulsed EPR experiments fail to detect the interaction of the magnetic nuclei of thallous ions, a monovalent cation activator as efficient as K^+ ion, with the unpaired electron in the inhibitor-derived *cis*-ethanesemidione radical.[45] However, it is not clear whether this conclusion is applicable to the case of catalytic reaction because their interactions with a substrate-derived radical has not been reported. We considered that the coordination of the substrate OH groups to K^+ ion is maintained during the course of the reaction because to fix substrates and intermediates in proper positions through the coordination to K^+, together with hydrogen bonds to the active-site residues, would be important for the stereospecific hydrogen abstraction and the stereoselective hydrogen recombination. The spin density on the K^+ ion was calculated to be almost zero (0.0) with either the previous simple model[6] or the present whole-enzyme model. Since K^+ ion exists hydrated in aqueous solution, some water molecules would be removed upon binding to the active site. The X-ray structures revealed that two water molecules remain bound directly to the K^+ ion at the active

(36) (a) Brownstein, A. M.; Abeles, R. H. *J. Biol. Chem.* **1961**, *236*, 1199. (b) Zagalak, B.; Frey, P. A.; Karabatsos, G. L.; Abeles, R. H. *J. Biol. Chem.* **1966**, *241*, 3028.
(37) (a) Rétey, J.; Umani-Ronchi, A.; Seibl, J.; Arigoni, D. *Experientia* **1966**, *22*, 502. (b) Rétey, J.; Umani-Ronchi, A.; Arigoni, D. *Experientia* **1966**, *22*, 72.
(38) Halpern, J.; Kim, S. H.; Leung, T. W. *J. Am. Chem. Soc.* **1984**, *106*, 8317.
(39) Hay, B. P.; Finke, R. G. *J. Am. Chem. Soc.* **1986**, *108*, 4820.
(40) (a) Hansen, L. M.; Kumar, P. N. V. P.; Marynick, D. S. *Inorg. Chem.* **1994**, *33*, 728. (b) Hansen, L. M.; Derecskei-Kovacs, A.; Marynick, D. S. *J. Mol. Struct. (THEOCHEM)* **1998**, *431*, 53.
(41) (a) Andruniow, T.; Zgierski, M. Z.; Kozlowski, P. M. *J. Phys. Chem. B* **2000**, *104*, 10921. (b) Andruniow, T.; Zgierski, M. Z.; Kozlowski, P. M. *Chem. Phys. Lett.* **2000**, *331*, 509. (c) Andruniow, T.; Zgierski, M. Z.; Kozlowski, P. M. *J. Am. Chem. Soc.* **2001**, *123*, 2679. (d) Kozlowski, P. M. *Curr. Op. Chem. Biol.* **2001**, *5*, 736. (e) Freindorf, M.; Kozlowski, P. M. *J. Am. Chem. Soc.* **2004**, *126*, 1928.
(42) Jensen, K. P.; Ryde, U. *J. Mol. Struct. (THEOCHEM)* **2002**, *585*, 239.
(43) Dolker, N.; Maseras, F. Lledos, A. *J. Phys. Chem. B* **2001**, *105*, 7564.
(44) Rovira, C.; Kunc, K.; Hutter, J.; Parinello, M. *Inorg. Chem.* **2001**, *40*, 11.
(45) Schwartz, P.; LoBrutto, R.; Reed, G. H.; Frey, P. A. *Helv. Chim. Acta* **2003**, *86*, 3764.

site of the substrate-free form of diol dehydratase.[3c] However, if we assume that K^+ ion in the active site remains coordinated to the substrate and all radical intermediates throughout the course of the reaction, the removal of K^+ ion from solvation upon binding to the enzyme would not affect the rate of catalysis, because the energetic change takes place in the process of K^+ binding, but not in the catalytic process. Besides the coordination to K^+ ion, the O1 atom of substrate is hydrogen bonded to the COO^- moiety of Glu170 and NH of Gln296, and the O2 atom to COO^- of Asp335. Moreover, the O2 atom of the substrate is hydrogen-bonded to His143. The strength of the hydrogen-bonding interaction is dependent on the protonation state of His143. In the protonated His143 model, the cationic imidazolium ion of His143 strongly attracts the O2 atom of the substrate, the distance of the hydrogen bond being 1.667 Å. In the unprotonated His143 model, the hydrogen atom connected to ϵ-nitrogen (Nϵ2) of HIE interacts with the O2 atom via a weaker hydrogen bond of 1.926 Å, but the side chain of HID has no hydrogen atom that can form a hydrogen bond to the O2 atom of the substrate. This hydrogen-bonding interaction has important influences on the structure of the hydrogen-bonding network. In particular, a significant change is observed in the distance between the OH group and Asp335; 1.573, 1.671, and 1.712 Å in the protonated His143, HIE, and HID models, respectively. The distance between the *pro-S* hydrogen and the C5′ carbon of adenosyl radical is also significantly changed, which is expected to have an impact on the activation energy for the following hydrogen abstraction step.

In a previous study,[6] we considered the interconversion between two possible conformations I and II as shown in Figure 4B, using a simple model involving only K^+ ion and (*S*)-1,2-propanediol. The activation energy from I to II is only 4.1 kcal/mol, and as opposed to our expectation, conformation II is 1.5 kcal/mol more stable than conformation I seen in the crystal structure.[6] However, the QM/MM optimized structures show that the surrounding amino acid residues stabilize conformation I via the hydrogen bonds to the OH groups of the substrate. The anionic (Glu170 and Asp335) and cationic (His143 of the protonated model) amino acid residues strongly attract the OH groups of the substrate, as indicated by the short hydrogen bonds between the residues and the substrate. These interactions would not allow the conformational change of substrate from I to II, in contrast to the earlier simple model. Thus, it is evident that the hydrogen-bonding network makes the *pro-S* hydrogen atom come into close contact with C5′ of the adenosyl group in conformation I.

3-3. Hydrogen Abstraction. Figures 5 and 6 show optimized geometries of the intermediates and transition states for the hydrogen abstraction and the OH group migration steps in the protonated and unprotonated His143 model (HIE), respectively. Although here we present only K^+ ion, the substrate, the ribose moiety, His143, and Glu170 for clarity, the optimized structure of the reactant complex has K^+ ion seven-coordinated by five oxygen atoms from amino acid residues and two oxygen atoms of the hydroxy groups of substrate as the crystal structure. Table 1 lists key geometrical features and energies of six points along the hydrogen atom abstraction in the protonated His143 model. Point 1 corresponds to the optimized structure of the reactant complex (C5′−H = 2.344 Å). Starting from point 1, we obtained the structures of points 2−5 by the partial optimization under the constraint of the C5′−H bond distance. At first, the potential energy is increased by the decrease of the C5′−H bond distance. The partially optimized structures of these points show that the C1−H bond distance increases as the C5′−H bond distance decreases and that the transition state for the hydrogen transfer is close to point 3.[46] The activation barrier of 15 kcal/mol for the hydrogen atom transfer is 6 kcal/mol higher than the corresponding barrier calculated in previous studies using the simple model.[4−6] This is mainly because we separately calculated the reactant complex and radical species in the previous study, whereas there is an additional stabilization energy in the reactant complex of the present realistic model, due to the weak interaction between the C1 and C5′ atoms. This is suitable for the stereospecific hydrogen atom transfer. In the simple model, we cannot reproduce such interactions between 1,2-propanediol and ethyl radical because the ethyl radical freely moves and collapses into an unreasonable structure for the hydrogen atom transfer. The protein environment, especially the adenine-binding pocket that anchors the adenosyl radical, plays an important role in positioning the radical species as discussed in section 3−1. In addition, we did not consider the free energy of the entire protein, which can lead to the reduction of the barrier height for hydrogen transfer (2−4 kcal/mol).[47] The release of the constraint on the C5′-H and C1−H bonds at point 5 leads to 1,2-diol radical (point 6) with no barrier. We also located the transition state for the hydrogen atom abstraction of the unprotonated His143 model (HIE) in the same procedure, as listed in Table 2. The estimated activation barrier for the hydrogen atom abstraction is 13.6 kcal/mol (the relative energy of point 3).

In the resultant 1,2-diol radical, several structural changes are observed compared with the reactant complex. A remarkable change is the hydrogen bond between the spectator OH group and Glu170; the O1−H bond distance increases by 0.036 (0.035) Å and the O (Glu170)-H bond distance decreases by 0.138

Table 1. Geometries and Energies of Points 1−6 along the Hydrogen Atom Abstraction Process in the Protonated His143 Model at the B3LYP/(6-31G* and 3-21G) Level of Theory

	point label					
	1	2	3	4	5	6
C1−H	1.100	1.272	1.297	1.312	1.325[a]	2.280
C5′−H	2.344	1.450[a]	1.430[a]	1.420[a]	1.400[a]	1.093
energy	0.0	14.3	15.4	15.3	14.4	−12.8

[a] Distance is constrained during geometry optimization. All distances and energies in the table are expressed in Å and kcal/mol, respectively.

Table 2. Geometries and Energies of Points 1−6 along the Hydrogen Atom Abstraction Process in the Unprotonated His143 Model (HIE) at the B3LYP/(6-31G* and 3-21G) Level of Theory

	point label					
	1	2	3	4	5	6
C1−H	1.103	1.281	1.298	1.316	1.371	2.658
C5′−H	2.621	1.470[a]	1.460[a]	1.450[a]	1.430[a]	1.091
energy	0.0	13.1	13.5	13.1	13.1	−9.8

[a] Distance is constrained during geometry optimization. All distances and energies in the table are expressed in Å and kcal/mol, respectively.

(46) In general, vibrational analyses are required to confirm that an optimized geometry corresponds to a transition state that has only one imaginary frequency. However, rigorous proofs are not possible because calculations of Hessian for the whole-enzyme model are beyond the practical reach.
(47) Gao, J.; Truhlar, D. G. *Annu. Rev. Phys. Chem.* **2002**, *53*, 467.

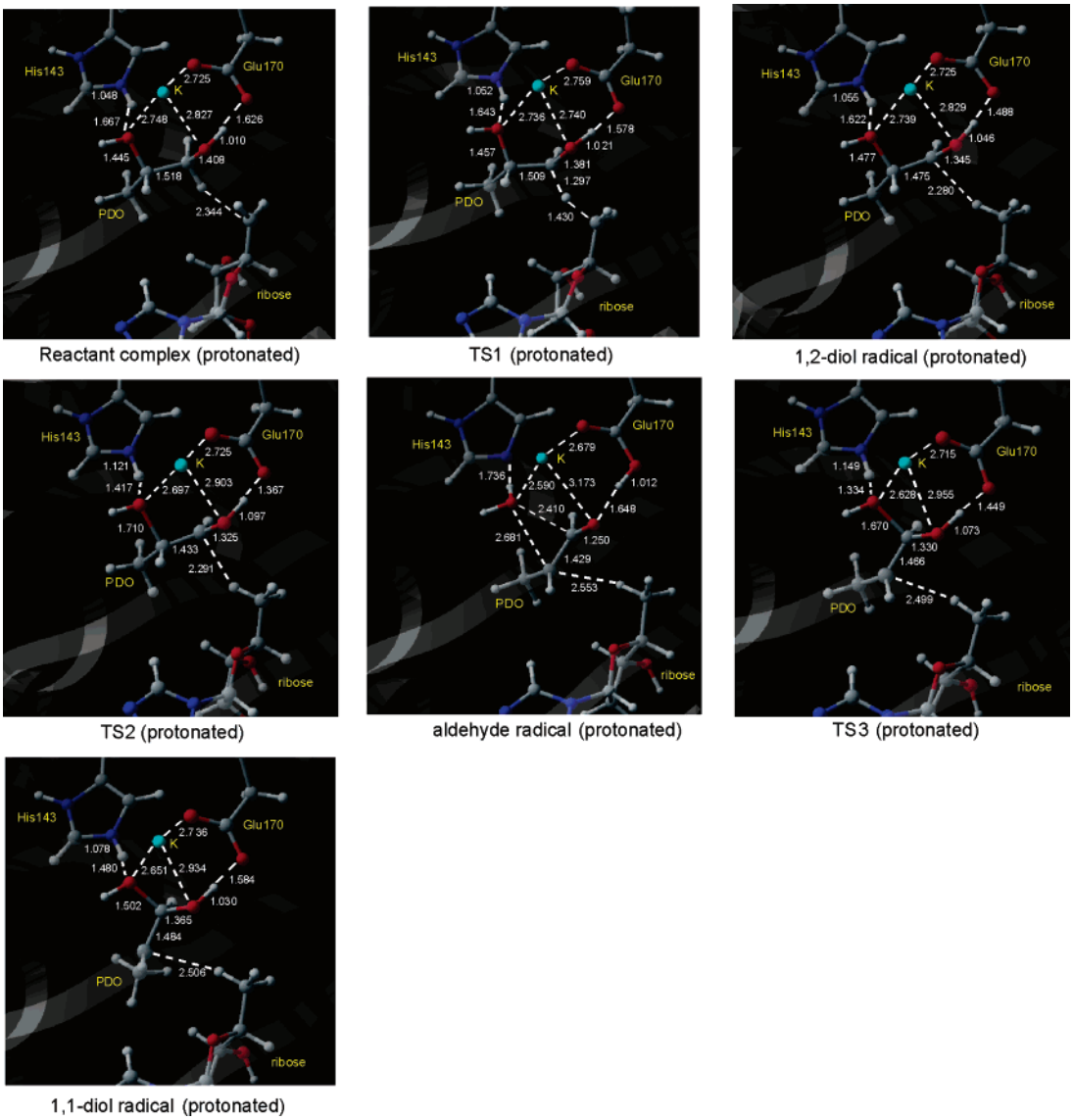

Figure 5. Optimized geometries of the intermediates and transition states for the hydrogen abstraction and the OH group migration in the protonated His143 residue model. Bond distances in Å.

(0.125) Å in the protonated His143 (unprotonated Hie143) model. This intermediate is an α-hydroxy radical species, which is up to 10^5 times more acidic than corresponding alcohols.[48−50] The anionic carboxyl group of Glu170 attracts the partially activated hydroxyl proton of the 1,2-diol radical. The relative energy of 1,2-diol radical of the protonated His143 (unprotonated Hie143) model is 6.0 (3.6) kcal/mol lower than the corresponding energy calculated with the simple model, mainly due to the acid−base interaction with Glu170. The bond distance of C1−O1 decreases from 1.408 (1.410) Å in the reactant complex to 1.345 (1.348) Å in the protonated His143 (unprotonated Hie143) model. This geometrical change is probably due to the resonance structure possessing O-centered radical and the concomitant C1−O1 double bond, as discussed previously.[6]

3-4 OH Group Migration. Smith, Golding, and Radom proposed that the OH group migration proceeds in a concerted manner and that the barrier height is lowered by a push−pull mechanism through partial protonation/partial deprotonation.[10d] We also reported using the simple model that the transition state for the concerted pathway has an activation energy of 18.7 kcal/mol for the OH group migration and that it is lowered only by 2.2 kcal/mol in the presence of K^+ ion.[4−6] We considered such a concerted OH group migration in this QM/MM calculations using whole-enzyme models of the diol dehydratase−AdoCbl complex with protonated and unprotonated His143 in the QM region. Although the ionization states of Glu170 and His143 are unknown at present, we assumed that Glu170 is ionized under the reaction conditions (pH 8.0). This assumption would be reasonable as judged from the X-ray structure of the enzyme because Glu170 at the active site is located in rather polar environment. Our calculational results show that the OH group migration step in the unprotonated His143 models proceeds in a similar concerted way, while the protonated His143 inevitably brings about the full protonation of the migrating OH group, leading to the production of an energetically stable aldehyde radical intermediate involving a water molecule and aldehyde radical species. Therefore, the OH group migration of the

(48) Buley, A. L.; Norman, R. O. C.; Pritchett, R. J. *J. Chem. Soc. B* **1966**, 849.
(49) Gilbert, B. C.; Larkin, J. P.; Norman. R. O. C. *J. Chem. Soc. Perk. Trans. II* **1972**, 794.
(50) Hayon, E.; Simic, M. *Acc. Chem. Res.* **1974**, *7*, 114.

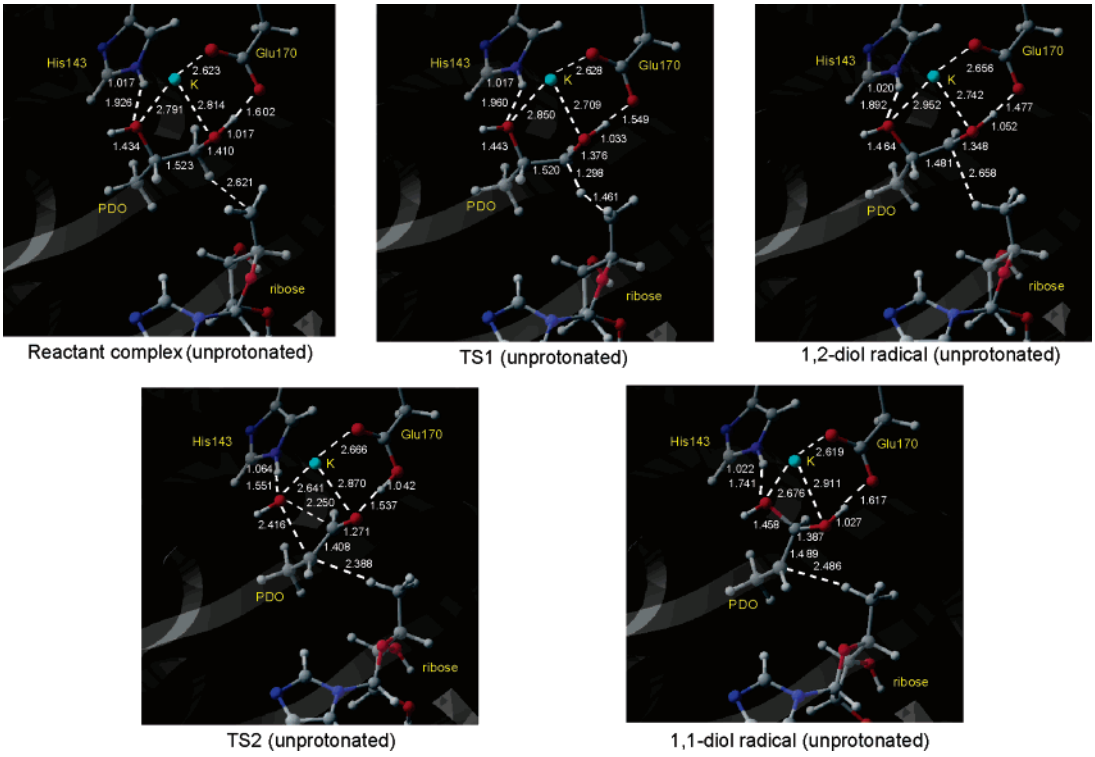

Figure 6. Optimized geometries of the intermediates and transition states for the hydrogen abstraction and the OH group migration in the unprotonated His143 model (HIE). Bond distances in Å.

Table 3. Geometries and Energies of Points 1−5 along the Conversion Process of 1,2-Diol Radical to Aldehyde Radical in the Protonated His143 Model at the B3LYP/(6-31G* and 3-21G) Level of Theory

	point label				
	1	2	3	4[b]	5
C2−O (OH)	1.477	1.700[a]	1.710[a]	1.720[a]	2.681
H (His143)-O (OH)	1.622	1.424	1.417	−	0.987
N (His143)-H	1.055	1.117	1.121	−	1.736
energy	−12.8	−6.4	−6.2	−	−25.3

[a] Distance is constrained during geometry optimization. [b] At this point barrierless collapse toward aldehyde radical intermediate occurs. All distances and energies in the table are expressed in Å and kcal/mol, respectively.

protonated His143 model should occur in a two-step manner in contrast to the previous studies. In this section, we would like to discuss this important difference in the OH group migration between the protonated and unprotonated His143 models from energetic, structural, and electronic points of view.

In the protonated His143 model, the OH migration begins with the full protonation of the migrating OH group by the imidazolium ion of His143. To estimate the activation energy of the proton transfer in a similar way to that used in obtaining the activation energy of TS1, we considered several intermediate steps from 1,2-diol radical intermediate (the first point) to aldehyde radical intermediate (the last point) using the partial optimization with the constraint of the O−C2 bond distance, as listed in Table 3. At first, the O−C2 bond activation raises the relative energy of the intermediate points, and at point 4 the synchronous proton transfer occurs as a result of the cleavage of the N−H bond and the O−H bond (spectator OH group) to produce a water molecule and aldehyde radical species. In this process the COO^- group of Glu170 temporarily accepts a proton from the spectator OH group to effectively form the aldehyde radical species. The release of the constraint on the O−C2 bond distance at point 4 leads to the aldehyde radical at point 5. The proton transfer from the protonated His143 is considered to promote the heterolytic cleavage of the C−O bond and the O−H bond, which drastically reduces the activation barrier for the C−O bond cleavage to 5.6 kcal/mol. A significant energy over 20 kcal/mol is released in the course of this dehydration process. This value is nearly identical to that of the computed heat of reaction (17.9 kcal/mol) for dehydration of 1,2-dihydroxypropyl radical at the B3LYP/6-311++G** level of theory. The stabilization by the production of the stable aldehyde radical species leads to a marked increase in activation energy for hydrogen recombination.[5,6,10] Although the produced aldehyde radical species has only one oxygen atom that can coordinate to K^+ ion, it is anchored to the active site via weak interactions. For example, protonated Glu170 attracts the carbonyl group of the aldehyde radical. The C−C−C backbone of the aldehyde radical is also fixed through van der Waals interactions with the surrounding water molecule and the ribose moiety of adenosyl radical.

In the next process, the produced water molecule attacks the C1 atom to recombine with the aldehyde radical species; proton transfers synchronously occur to reproduce the protonated form of His143 and the spectator OH group (Table 4). The activation barrier for the process is estimated to be 18.9 kcal/mol, the value of which is as high as that for the OH group migration in the simple model without amino acid residues. The produced 1,1-diol radical intermediate is 15.8 kcal/mol unstable compared with the aldehyde radical intermediate.

On the other hand, the OH group migrates to form 1,1-diol radical via a transition state with a triangle structure in the unprotonated His143 models. In these models, the activation barrier for the OH migration is lowered mainly by deprotonation

Table 4. Geometries and Energies of Points 1−7 along the Conversion Process of Aldehyde Radical to 1,1-Diol Radical in the Protonated His143 Model at the B3LYP/(6-31G* and 3-21G) Level of Theory

	point label						
	1	2[b]	3	4	5	6	7
C1−O (OH)	2.410	1.680[a]	1.670[a]	1.660[a]	1.650[a]	1.620[a]	1.502
H (His143)-O (OH)	0.987		1.334	1.347	1.372	1.400	1.480
N (His143)-H	1.736		1.490	1.140	1.127	1.112	1.078
energy	−25.3		−7.8	−8.1	−8.5	−9.2	−11.5

[a] Distance is constrained during geometry optimization. [b] At this point barrierless collapse toward aldehyde radical intermediate occurs. All distances and energies in the table are expressed in Å and kcal/mol, respectively.

Table 5. Geometries and Energies of Points 1−7 along the Conversion Process of 1,2-Diol Radical to 1,1-Diol Radical in the Unprotonated His143 Model (HIE) at the B3LYP/(6-31G* and 3-21G) Level of Theory

	Point label						
	1	2	3	4	5	6	7
C1−O	2.375	2.300[a]	2.250[a]	2.200[a]	2.100[a]	1.900[a]	1.458
C2−O	1.464	2.394	2.416	2.441	2.476	2.492	2.392
energy	−9.8	3.9	4.2	3.7	3.0	0.6	−12.2

[a] Distance is constrained during geometry optimization. All distances and energies in the table are expressed in Å and kcal/mol, respectively.

Table 6. Geometries and Energies of Points 1−5 along the Conversion Process of 1,2-Diol Radical to 1,1-Diol Radical in the Simple Model

	point label					
	1	2	3	4	5	exact[b]
C1−O	2.573	2.526	2.466	2.300[a]	2.200[a]	2.296
C2−O	2.300[a]	2.350[a]	2.375[a]	2.378	2.538	2.373
energy	20.1	20.4	20.5	20.6	20.2	20.6

[a] Distance is constrained during geometry optimization. [b] The structure of transition state is located by full optimization. All distances and energies in the table are expressed in Å and kcal/mol, respectively.

of the spectator OH group because unprotonated His143 cannot act as an effective proton donor. The pull mechanism has been considered to have only a minor impact on the stabilization of the transition state for the OH group migration without the aid of the push effect of His143. However, QM/MM calculations revealed that the pull effect of Glu170 is more important in the reduction of the activation barrier for the OH group migration (1.6 kcal/mol by His143 and 5.6 kcal/mol mainly by Glu170, as described below). We estimated the activation barrier of the OH group migration in the unprotonated His143 models using partial optimization with the constraint of the O−C1 bond distance. Table 5 shows that point 3 is close to the transition state for the OH group migration in the HIE model. The estimated activation barrier for this process is 11.5 kcal/mol, the value of which is 7.2 kcal/mol lower than that in the simple model. To confirm the reliability of this method for transition state search, we recalculated the transition state for the OH group migration in the simple model in a way similar to the QM/MM optimization procedure for TS2. As listed in Table 6, the estimated structure of the transition state is very similar to the fully optimized one, the energetical deviation from the fully optimized structure being less than 0.1 kcal/mol. We compared the energy profiles of the HIE and HID models to quantitatively evaluate the catalytic effects of the Glu170 and the unprotonated His143 residues. In the HID model, there is no hydrogen-bonding interaction between the O2 atom of the substrate and His143, the bond distance between ϵ-nitrogen (Nϵ2) atom of His143 and the migrating OH group being 3.022 Å in the 1,2-diol radical species, as discussed in section 3−2. The transition state for the OH group migration in this model also has a triangle structure; the C−C bond distance is 1.417 Å, and the C−O1 and C−O2 bond distances are 2.100 Å and 2.396 Å, respectively. The activation barrier for this step is calculated to be 13.1 kcal/mol, the value of which is 5.6 kcal/mol lower than that in the simple model. This barrier reduction is mainly responsible for the pull effect of Glu170, which is consistent with the report[10] of Smith, Golding, and Radom that the pull effect of $HCOO^-$ is able to reduce the barrier of the OH migration of 1,2-dihydroxyethyl radical by 5.7 kcal/mol. It is suggested from our calculations that Glu170 accepts the proton of O1−H in the transition state for the OH group migration (TS2) in both protonated and unprotonated His143 models (Figures 5 and 6). The p*K*a value for 1,2-diol radical (substrate radical) is estimated to be ∼12,[50] but the coordination of OH group to K^+ ion (Lewis acid) would lower its p*K*a. Electrostatic stabilization of oxyanion by K^+ ion in TS2 might further facilitate the dissociation of O1−H, resulting in the proton transfer from O1−H to the $-COO^-$ group of Glu170 in the transition state. In the reverse reaction from 1,1-diol radical (product radical) to 1,2-diol radical, the proton transfer from the OH group to Glu170 would occur similarly in the transition state. Moreover, we can predict from the difference between the activation energy of TS2 for HIE and HID that the hydrogen-bonding interaction between the O2 atom of the substrate and unprotonated His143 lowers the activation barrier by 1.6 kcal/mol, which corresponds to a 13-fold rate acceleration at 37 °C. This result is consistent with the mutational studies indicating that the His143Gln and His143Ala mutations lead to a 5- and 69-fold lowering in the rate constant for the dehydration reaction, respectively. A significant change is also observed in the relative energy of 1,1-diol radical; the 1,1-diol radical species lies 5.1 kcal/mol above the 1,2-diol radical species in the HID model, while the 1,1-diol radical species lies 2.0 kcal/mol below the 1,2-diol radical species in the HIE model. The hydrogen-bond distance of the 1,1-diol radical species is 0.151 Å shorter than that of the 1,2-diol radical species. These results indicate that His143 contributes to the stabilization of the 1,1-diol radical species via the hydrogen-binding interaction. In summary of the discussion on the unprotonated His143 models, we conclude that the barrier reduction induced by the Glu170 residue is 3.5 times larger than that by the His143 residue although the unprotonated His143 residue affects the reaction rate of the OH group migration process to some extent as mutational studies suggested.

3-5 Is the His143 Residue Protonated or Not? In view of the calculated energetic profiles depicted in Figure 7, the reaction pathway with unprotonated His143 seems to be kinetically more favorable than that with protonated His143 for the AdoCbl-

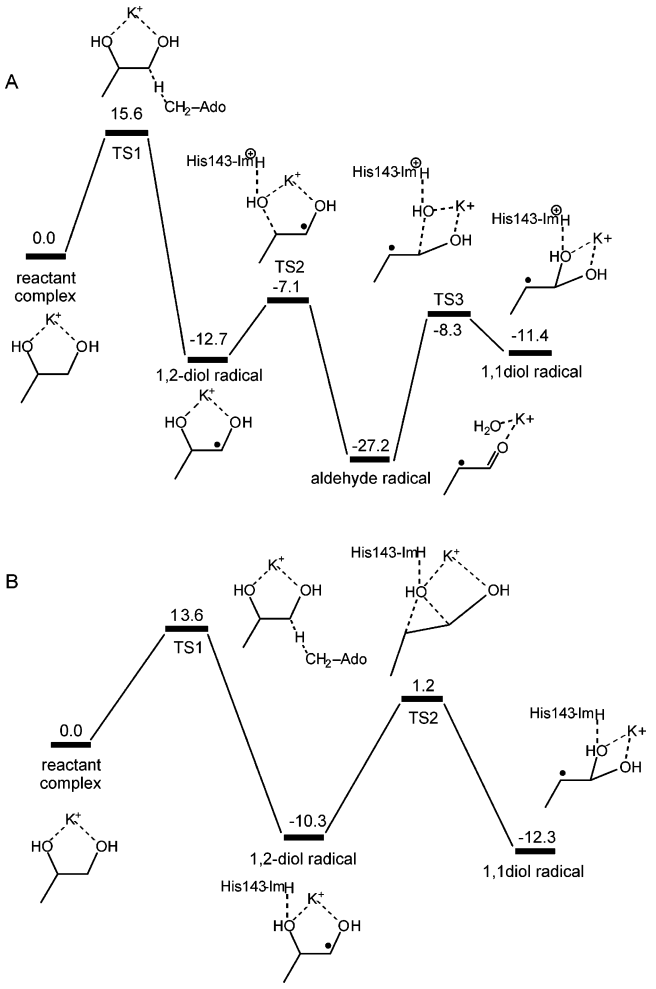

Figure 7. Energy diagrams for the hydrogen abstraction and the OH migration in the protonated His143 (A) and unprotonated Hie143 (B) models. Energies in kcal/mol.

dependent dehydration. George et al.[51] concluded from observed rate constants that any dissociation process that has an energy exceeding about 15 kcal/mol can be disregarded as a potential step in the diol dehydratase pathway. This statement is satisfied with all the transition states but TS3 in both reaction pathways. Which pathway is more likely in the diol dehydratase-mediated dehydration? Semialjac and Schwarz proposed intriguing functions of histidine depending on pH values in the active site of ethanolamine ammonia-lyase; in the range $6 < pH < 9.5$, the Nϵ2 atom of the histidine residue is not protonated as a result of the full protonation of substrate by the histidine residue.[52,53] The present QM/MM calculations with protonated His143 are in good agreement with their proposal. The 1,2-diol radical intermediate is converted to the aldehyde radical intermediate by the proton transfer from His143 to the migrating OH group in the QM/MM calculation. A stable aldehyde radical species is produced by the synergistic interplay of the protonation of the migrating OH group and the deprotonation of the spectator OH group with the aid of His143 and Glu170. The stabilization energy of 14.5 kcal/mol released in the course of the proton-transfer process supports the proposal by Semialjac and Schwarz.

Scheme 1

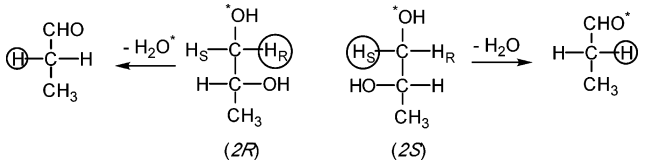

The following recombination process of the migrating OH group to C1 is found to proceed in a manner similar to the OH migration step that they reported. However, several experimental results can rule out the pathway including protonated His143. The energy barrier for the hydrogen abstraction in the protonated His143 model is lower than that for the hydration of aldehyde radical to 1,1-diol radical (Figure 7A). This is not consistent with the experimental finding that the hydrogen abstraction is the rate determining step for the overall reaction.[7−9] Recently, Toraya and co-workers synthesized ^{13}C-labeled 1,2-propanediols and measured EPR spectra using them as substrates.[54] A distinct change in the hyperfine splitting was observed with [1-^{13}C]1,2-propanediol, whereas the EPR spectra with [2-^{13}C]1,2-propanediol remains essentially unchanged from normal 1,2-propanediol. This experimental result clearly indicates that the organic radical species observed by EPR is the C1-centered radical. The calculated energy profile of the protonated His143 model disagrees with the conclusion from the EPR measurements because the overwhelmingly stable aldehyde radical species should be detected instead of 1,2-diol radical species in the reaction mechanism. Moreover, direct production of aldehyde from the aldehyde radical intermediate is likely to occur without the OH migration process in the protonated His143 model because the C2 atom of the aldehyde radical species is in close contact with the ribose moiety, the distance between the C2 atom of aldehyde radical species and a hydrogen atom of the ribose moiety being 2.553 Å. We reported in the previous papers that the transition state for the hydrogen recombination of 1,1-diol radical species lies 14.8 kcal/mol above that of aldehyde radical intermediate.[5,6] Despite the energetical feasibility of the direct aldehyde production, the mechanism is also inconsistent with experimental results. Abeles's[36] and Rétey's[37] groups established the stereochemistry of the diol dehydratase reaction by the labeling experiments, as shown in Scheme 1. The *pro-S* and *pro-R* hydrogen atoms are specifically abstracted from (*S*)- and (*R*)-1,2-propanediol, respectively, and migrate to C2, as discussed above. The dehydration is also controlled by the enzyme; only one of the two OH groups on the substrate is eliminated. The O atom of the product water comes from O1 when (*R*)-1,2-propanediol is used as substrate, but does not come from O1 when (*S*)-1,2-propanediol is used. The direct mechanism of aldehyde production is inconsistent with the stereospecific dehydration because the oxygen atom of the product water always originates from the O2 atom, which is hydrogen-bonded to His143 in the protonated His143 model.

On the other hand, the energy profile for the hydrogen abstraction and the OH migration process of the unprotonated His143 model clearly explains the experimental findings. In this model, the aldehyde radical species is not formed because no proton donor exists near the migrating OH group and the hydrogen of the spectator HO group is tightly bound, due to

(51) George, P.; Glusker, J. P.; Bock, Ch. W. *J. Am. Chem. Soc.* **1997**, *119*, 7065.
(52) Semialjac, M.; Schwarz, H. *J. Am. Chem. Soc.* **2002**, *124*, 8974.
(53) Semialjac, M.; Schwarz, H. *J. Org. Chem.* **2003**, *68*, 6967.
(54) Yamanishi, M.; Ide, H.; Murakami, Y.; Toraya. T. submitted.

the hydrogen-bonding interaction with Glu170. Preliminary calculations suggest that the aldehyde radical intermediate lies about 12 kcal/mol above the 1,2-diol radical when a proton is transferred from the spectator OH group to the migrating OH group. Although the rate of the diol dehydratase reaction was reported to be constant in the wide range of pH from 6.0 to 10.0,[34] *k*cat/*K*m showed a bell-shaped pH-dependence curve with the maximum at 8.0 and half-maximums around 6.5 and 9.5 (data not shown). This is consistent with the idea that the enzyme with unprotonated His143 is active. Moreover, the relative energy of the transition state for the hydrogen abstraction process is higher than that for the OH migration in this pathway, which is consistent with the observed large KIEs that indicate the cleavage of C−H bond in the rate-determining step.[7−9] This result is in good agreement with our proposal that the active-site amino acid residues significantly lower the energy of the transition state of the OH group migration.[4−6] The stereochemistry of the diol dehydratase reaction shown in Scheme 1 has recently been explained without the involvement of aldehyde radical intermediate on the basis of the X-ray structures of (*R*)- and (*S*)-1,2-propanediol-bound forms of diol dehydratase−cyanocobalamin complexes.[3d] For these reasons, we predict that the OH group migration in diol dehydratase proceeds by the concerted mechanism in the absence of protonated His143. This prediction is based on the assumptions of (i) the ionization of Glu170 and (ii) the coordination of the substrate and all radical intermediates to K^+ ion.

4. Conclusions

We presented a theoretical study of the hydrogen abstraction and the OH group migration mediated by diol dehydratase using a quantum mechanical/molecular mechanical (QM/MM) method. Optimized geometries of the intermediates and transition states involving about 13 500 atoms describe important functions of the active-site amino acid residues in the catalytic mechanism. As suggested from a modeling study of the crystal structure of the diol dehydratase−AdePeCbl complex, the hydrogen-bonding interactions between the adenine ring and the surrounding amino acid residues accelerate the cleavage of the Co−C bond and control the access of the adenosyl radical to the *pro-S* hydrogen atom of (*S*)-1,2-propanediol by the rotation of the ribose moiety around the glycosidic linkage for the stereospecific hydrogen abstraction. At the substrate-binding site four amino acid residues, His143, Glu170, Gln296, and Asp335, are hydrogen-bonded to the substrate in addition to K^+ ion. The activation energy for the hydrogen abstraction is estimated to be 15.6 (13.6) kcal/mol in the protonated His143 (unprotonated Hie143) model. We found a significant difference in the mechanism of the OH group migration in the protonated and unprotonated His143 models. In the protonated His143 model, the OH migration begins with the full protonation of the migrating OH group by the protonated His143 residue. The formation of the aldehyde radical species takes place in a synergistic interplay of protonation and deprotonation of the OH groups by His143 and Glu170. After that, 1,1-diol radical species is formed by the recombination of the produced water molecule and aldehyde radical. On the other hand, the OH group migration proceeds in a concerted manner through a triangle transition state in the unprotonated His143 models. The latter mechanism seems to be kinetically more favorable than the former one from the energetic point of view and is consistent with the results of EPR measurements and labeling experiments as well as the pH-activity profile. We considered two unprotonated models: HIE model with a hydrogen atom at ϵ-nitrogen (Nϵ2) and HID model with a hydrogen atom at δ-nitrogen (Nδ1). The HID model has no hydrogen-bonding interaction between the O2 atom of the substrate and His143, and therefore the decrease of the activation barrier for the OH group migration step is mainly due to the pull effect of Glu170 in this model (5.6 kcal/mol). The barrier reduction of the OH migration step by the push effect of His143 is evaluated to be 1.6 kcal/mol from the difference in the activation barrier between the HIE and HID models. On the basis of the assumptions on the basis of the assumptions of (i) the ionization of Glu170 at the start of the reaction and (ii) the coordination of the substrate and all radical intermediates to K^+ ion throughout the course of the reaction, it is predicted that the His143 residue is not protonated and that the pull effect of Glu170 is the most important factor that reduces the activation barrier of the OH migration in the diol dehydratase-catalyzed dehydration reaction in contrast to the previous studies by Smith, Golding, and Radom.

Acknowledgment. K.Y. acknowledges the Ministry of Culture, Sports, Science and Technology of Japan, the Japan Society for the Promotion of Science, Japan Science and Technology Cooperation, the Takeda Science Foundation, and Kyushu University P & P "GreenChemistry" for their support of this work. K.Y. also thanks Prof. H. M. Marques for providing amber parameters for cobalamin. This study was supported in part by a Grant-in-Aid for Scientific Research on Priority Areas (No. 753) to T.T. and K.Y. as well.

Supporting Information Available: Two tables and two figures of the unprotonated His143 model (HID), one table of single-point calculations and one table of amber parameters for cobalamin. This material is available free of charge via the Internet at http://pubs.acs.org.

JA045572O